Physics and Imaging in Radiation Oncology 21 (2022) 72–77

Contents lists available at ScienceDirect

Physics and Imaging in Radiation Oncology

journal homepage: www.sciencedirect.com/journal/physics-and-imaging-in-radiation-oncology

Original Research Article

# A positron emission tomography radiomic signature for distant metastases risk in oropharyngeal cancer patients treated with definitive chemoradiotherapy

N. Patrik Brodin [a,b,*], Christian Velten [a,b], Jonathan Lubin [b], Jeremy Eichler [b], Shaoyu Zhu [c], Sneha Saha [c], Chandan Guha [a,b,d,e], Shalom Kalnicki [b,d], Wolfgang A. Tomé [a,b,f], Madhur K. Garg [a,b,d,g], Rafi Kabarriti [a,b,*]

[a] Institute for Onco-Physics, Albert Einstein College of Medicine, Bronx, NY, USA
[b] Department of Radiation Oncology, Montefiore Medical Center, Bronx, NY, USA
[c] Albert Einstein College of Medicine, Bronx, NY, USA
[d] Department of Urology, Montefiore Medical Center, Bronx, NY, USA
[e] Department of Pathology, Albert Einstein College of Medicine, Bronx, NY, USA
[f] Department of Neurology, Albert Einstein College of Medicine, Bronx, NY, USA
[g] Department of Otorhinolaryngology - Head & Neck Surgery, Montefiore Medical Center, Bronx, NY, USA

ARTICLE INFO

*Keywords:*
Radiomics
Positron emission tomography
Oropharyngeal cancer
Risk stratification

ABSTRACT

*Background and purpose:* Disease recurrence and distant metastases (DM) are major concerns for oropharyngeal cancer (OPC) patients receiving definitive chemo-radiotherapy. Here, we investigated whether pre-treatment primary tumor positron emission tomography (PET) features could predict progression-free survival (PFS) or DM.
*Methods and materials:* Primary tumors were delineated on pre-treatment PET scans for patients treated between 2005 and 2018 using gradient-based segmentation. Radiomic image features were extracted, along with SUV metrics. Features with zero variance and strong correlation to tumor volume, stage, p16 status, age or smoking were excluded. A random forest model was used to identify features associated with PFS. Kaplan-Meier methods, Cox regression and logistic regression with receiver operating characteristics (ROC) and 5-fold cross-validated areas-under-the-curve (CV-AUCs) were used.
*Results:* A total of 114 patients were included. With median follow-up 40 months (range: 3–138 months), 14 patients had local recurrence, 21 had DM and 38 died. Two-year actuarial local control, distant control, PFS and overall survival was 89%, 84%, 70% and 84%, respectively. The wavelet_LHL_GLDZM_LILDE feature slightly improved PFS prediction compared to clinical features alone (CV-AUC 0.73 vs. 0.71). Age > 65 years (HR = 2.64 (95%CI: 1.36–5.2), p = 0.004) and p16-negative disease (HR = 3.38 (95%CI: 1.72–6.66), p < 0.001) were associated with poor PFS. A binary radiomic classifier strongly predicted DM with multivariable HR = 3.27 (95% CI: 1.15–9.31), p = 0.027, specifically for patients with p16-negative disease with 2-year DM-free survival 83% for low-risk vs. 38% for high-risk patients (p = 0.004).
*Conclusions:* A radiomics signature strongly associated with DM risk could provide a tool for improved risk stratification, potentially adding adjuvant immunotherapy for high-risk patients.

## 1. Introduction

Oropharyngeal cancer (OPC) is one of the most common cancers of the head and neck, accounting for about 30% in the United States [1], with increasing incidence among younger patients [2]. Combined radiation therapy (RT) and chemotherapy are key components of definitive treatment. This is especially true for patients with human papilloma virus (HPV) p16-positive tumors, as these patients have promising prognoses following definitive treatment, with 3-year survival rates of about 80%, compared to around 60% for patients with

* Corresponding authors at: Institute for Onco-Physics, Albert Einstein College of Medicine and Montefiore Medical Center, 1300 Morris Park Ave, Block Building, Room 104, Bronx, NY 10461, USA.
*E-mail addresses:* patrik.brodin@einsteinmed.org (N.P. Brodin), rkabarri@montefiore.org (R. Kabarriti).

https://doi.org/10.1016/j.phro.2022.02.005
Received 29 September 2021; Received in revised form 7 February 2022; Accepted 11 February 2022

HPV-negative tumors [3–5]. Despite recent treatment advances, treatment-related toxicities still carry significant morbidity for these patients and local recurrence or distant metastases (DM) are a major concern [4,6–8].

The use of Fluorodeoxyglucose (FDG) positron emission tomography (PET) has become an important component of staging and treatment planning for OPC [9,10] with current research efforts examining the potential of using PET for prediction of treatment outcome [11–13]. With quantitative imaging biomarkers gaining popularity across the oncology field, there is definitely an evolving role of PET scans in the management of OPC. One such development is the derivation of radiomic image features, which are mathematical representations of the textural patterns of a three-dimensional image of a tumor.

As far as recent treatment adaptation is concerned, the focus has been on attempting to de-intensify the treatment in order to reduce toxicity, especially for patients with HPV p16-positive disease who are known to have better prognoses [14,15]. Among such efforts are several ongoing clinical trials aimed at reducing the dose of radiation for patients with HPV-associated OPC.

In our institution we see a large portion of patients from underserved communities typically underrepresented in clinical trials. Moreover, many of our patients with OPC often present with large tumors and advanced disease, which is associated with worse treatment outcome. In this study our aim was to investigate whether radiomic features of the primary tumor derived from pre-treatment FDG-PET scans were associated with progression-free survival (PFS) or DM. We hypothesized that a PET-based radiomics risk score could improve the risk stratification for these patients, beyond that of important clinical factors such as HPV p16 status.

## 2. Materials and methods

### 2.1. Patient selection

In this Institutional Review Board approved retrospective study, we included consecutive patients with oropharyngeal cancer treated with definitive RT and chemotherapy in our department between 2005 and 2018. Further inclusion criteria were a pre-RT FDG-PET scan showing some PET-avid disease in the primary tumor and a minimum follow-up of 3 months post RT. Patients who received post-operative adjuvant RT were not included.

### 2.2. Primary tumor segmentation and radiomic feature extraction

Primary tumors were identified in the pre-treatment attenuation-corrected PET scans using the information available from the patients' diagnostic work-up. Once identified, the primary tumor was segmented on the PET scan using the PET-edge function in MIM (MIM software Inc., Cleveland, OH). The PET-edge function, a gradient-based semi-automatic algorithm, was used to generate the primary tumor segmentations in order to make them less sensitive to inter-observer variations. The majority of the FDG-PET scans were acquired on a Philips GEMINI PET/CT scanner, with voxel size 4x4x4 $mm^3$ and reconstructed using an iterative time-of-flight algorithm (BLOB-OS-TF), with more details provided in supplementary table S1. Commonly used metrics including metabolic tumor volume (MTV), mean standardized uptake value ($SUV_{mean}$), $SUV_{max}$ and total lesion glycolysis (TLG) were tabulated from the tumor segmentations directly in MIM.

Radiomic features were generated using the RadiomiX toolbox (Radiomics, Liege, Belgium). PET scans with accompanying tumor contours were exported in DICOM format and pre-processed using isotropic resampling to $4 \times 4 \times 4$ $mm^3$ and z-score normalization to reduce the dependency on specific scanner type and reconstruction protocol. The image intensity was discretized into 32 separate bins. Radiomic features were calculated based on the pre-processed three-dimensional tumor region of interest (ROI) data, as well as its Laplacian of Gaussian (LoG) and wavelet convolutions using coiflet1 filtering. Features were calculated based on second order statistics, intensity histogram, local intensity, shape, gray-level co-occurrence matrix, gray-level run length matrix, gray-level size zone matrix, gray-level distance zone matrix, neighborhood gray-tone difference matrix, neighborhood gray-level dependence matrix and fractal dimension.

### 2.3. Statistical analysis

Radiomic features with zero variance, i.e. no variation in the value of a particular feature between different patients, were excluded from the analysis. Features with a strong correlation (Pearson's $r > 0.75$) to MTV, $SUV_{max}$, TLG, disease stage, gross tumor volume, HPV p16 status, smoking status or age were excluded from the analysis. Following this, features with strong cross-correlation (Pearson's $r > 0.75$) were eliminated, keeping the feature with the smallest average correlation with all other candidate features.

A random forest model with 500 classification trees was trained for predicting progression-free survival (PFS) on the remaining radiomic features using the *randomForest 4.6–14* R package. The ten most important radiomic features selected in the random forest model were then evaluated by individually adding each feature to a multivariable logistic regression model of PFS adjusted for known clinical prognostic variables (disease stage, age, HPV p16 status and smoking). Any radiomic features showing a significant association with PFS ($p < 0.05$) after adjusting for these clinical factors were included in the final radiomics risk signature. Included radiomic features were split into quartiles and assigned risk scores based on visual examination of the association with PFS in each quartile, from which a binary radiomics risk classifier grouped patients as either low-risk or high-risk.

Logistic regression models with 5-fold cross-validation were constructed to evaluate the classification performance of models using only clinical variables, SUV metrics, or radiomic features as well as clinical + SUV metrics or clinical + radiomic features. The areas under the receiver operating characteristics (ROC) curves with bootstrap bias corrected 95% confidence intervals were used to compare classification performance and Akaike information criterion (AIC) and Hosmer-Lemeshow tests to assess goodness-of-fit. Models were constructed on a complete case basis, with no imputation of missing data.

Kaplan-Meier methods with log-rank tests and Cox proportional hazards regression were used to examine the association with PFS, local control and distant control based on time from RT until end of follow-up. The reproducibility of the identified radiomic features was tested by an independent observer re-contouring the primary tumor ROIs for a subgroup of 30 randomly selected patients and re-computing the corresponding radiomic features. Statistical analyses were performed using R version 4.1.0 and STATA v.14 (StataCorp, College Station, TX), with $p < 0.05$ as the statistical significance threshold.

## 3. Results

One-hundred and fourteen patients were included in this analysis. The median follow-up was 40 months (range: 3 to 138 months) and the median time from PET scan to start of RT was 16 days (inter-quartile range: 11 to 40 days). The majority of patients were male (75%), about half of all patients had HPV p16-positive disease (56%) and a large proportion presented with stage IV disease (71%), with further details shown in Table 1. Fourteen patients had a local recurrence, 21 had DM and 38 patients died within the study period. The 2-year actuarial local control, distant control, PFS and overall survival was 89%, 84%, 70% and 84%, respectively.

A total of 4,442 radiomic features were calculated for each patient, with 4,221 features excluded that left 221 image features entered into the random forest model. The ten most important features identified in the random forest model are shown in supplementary fig. S1. Only the *wavelet_LHL_GLDZM_LILDE* radiomic feature was significantly associated

**Table 1**
Patient and treatment characteristics.

| | All patients (n = 114) |
|---|---|
| Age (y), median (range) | 62 (45, 88) |
| Gender, n (%) | |
| Male | 86 (75) |
| Female | 28 (25) |
| Stage, n (%) | |
| II | 14 (12) |
| III | 19 (17) |
| IV | 81 (71) |
| Smoking*, n (%) | |
| Yes | 82 (73) |
| No | 31 (27) |
| Chemotherapy, n (%) | |
| Yes | 99 (87) |
| No | 15 (13) |
| HPV p16 status** | |
| Positive | 56 (56) |
| Negative | 44 (44) |
| Gross tumor volume ($cm^3$), median (IQR) | 34.1 (23.9, 64.8) |
| Metabolic tumor volume ($cm^3$), median (IQR) | 16.1 (10.7, 29.1) |
| $SUV_{mean}$, median (IQR) | 6.6 (4.9, 8.6) |
| $SUV_{max}$, median (IQR) | 11.2 (8.5, 15.1) |

*Smoking status unavailable for 1 patient.
**HPV p16 status unavailable for 14 patients.
IQR – inter-quartile range.

with PFS (p = 0.021) after adjusting for clinical factors (cf. supplementary table S2). There was no significant association between this radiomic feature and any of the tabulated clinical variables (supplementary table S3) and no correlations were found with gross tumor volume or standard SUV metrics (supplementary fig. S2).

The classification performance of the logistic regression model for PFS based on clinical features was good with 5-fold cross-validated AUC (CV-AUC) of 0.71, with slight improvement when adding the radiomic feature (CV-AUC 0.73), cf. Table 2. Detailed results for the logistic regression models are provided in supplementary table S4. A lower AIC value (121.6 vs. 125.5) showed a better fit to the PFS data when including the radiomic feature, compared to clinical features alone. The model based on standard SUV metrics alone did not show good predictive performance (CV-AUV 0.57) and no improvement was seen when adding SUV metrics to the clinical features, resulting in a CV-AUC of 0.71. These results are further illustrated by the ROC curves shown in Fig. 1.

The median value of the *wavelet_LHL_GLDZM_LILDE* feature was 0.035 (inter-quartile range: 0.027 to 0.056). Following the quartile splits and visual examination (with distribution shown in supplementary fig. S3), risk points were assigned so that patients within the highest quartile of *wavelet_LHL_GLDZM_LILDE* (feature value > 0.056) were considered to have a high radiomics risk score, whereas those in the lowest three quartiles (≤0.056) were considered low-risk. This resulted in 86 patients

**Table 2**
Area under the receiver operating characteristics curves based on logistic regression models evaluating the classification performance of the different models to predict progression-free survival.

| Model | Apparent AUC (95% CI) | 5-fold cross-validated AUC (bootstrap bias corrected 95% CI) |
|---|---|---|
| Clinical features* | 0.76 (0.66, 0.85) | 0.71 (0.57, 0.80) |
| SUV metrics** | 0.62 (0.51, 0.72) | 0.57 (0.43, 0.67) |
| Radiomic feature | 0.66 (0.55, 0.77) | 0.67 (0.49, 0.73) |
| Clinical + SUV metrics | 0.78 (0.69, 0.88) | 0.71 (0.57, 0.80) |
| Clinical + Radiomic feature | 0.78 (0.70, 0.87) | 0.73 (0.59, 0.81) |

*HPV p16 status, Age, Smoking, Disease stage.
**Metabolic tumor volume, $SUV_{mean}$, $SUV_{max}$.

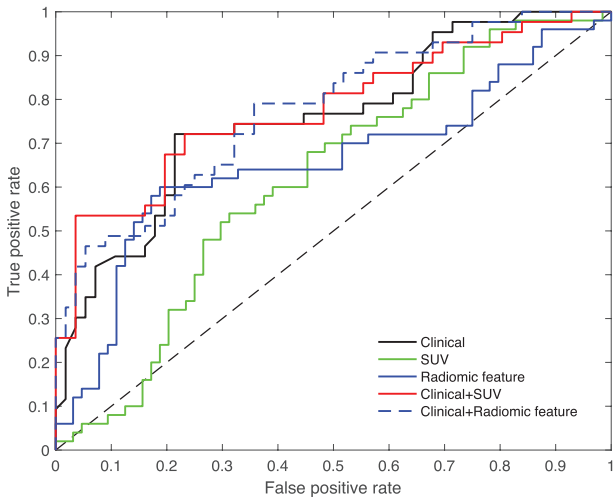


**Fig. 1.** Receiver operating characteristics curves comparing the classification performance of different logistic regression models predicting progression-free survival.

(75%) classified as low-risk and 28 patients (25%) classified as high-risk, with primary tumor segmentations from four example patients presented in supplementary fig. S4.

The Kaplan-Meier survival analysis identified a high radiomics risk score, age >65 years and HPV p16-negative disease to be associated with worse PFS, as illustrated in Fig. 2. Multivariable Cox proportional hazards regression identified age > 65 years (HR = 2.64 (95% CI: 1.36, 5.2), p = 0.004) and HPV p16 negative disease (HR = 3.38 (95% CI: 1.72, 6.66), p < 0.001) as significant predictors of poor PFS, while a high radiomics risk score was borderline significantly associated with PFS on multivariable analysis (HR = 1.79 (95% CI 0.93, 3.45), p = 0.081).

Analyzing the association of low vs. high radiomics risk score with the risk of local recurrence and DM separately showed that while a high radiomics risk score was not associated with local control (multivariable HR = 1.19 (95% CI: 0.27, 5.23), p = 0.81), it was strongly associated with increased risk of DM (multivariable HR = 3.27 (95% CI: 1.15, 9.31), p = 0.027). Importantly, a high radiomics risk score was associated with significantly increased risk of DM for patients with HPV p16-negative disease, but not for patients with HPV p16-positive disease (Fig. 3).

For patients with HPV p16-negative disease we found that the 2-year DM-free survival was 83% for patients with a low radiomics risk score, compared to 38% for high-risk patients (p = 0.004). Conversely, for patients with HPV p16-positive disease there was no significant difference between patients with low vs. high radiomics risk score with 2-year DM-free survival of 95% vs. 90%, respectively (p = 0.19).

In general, there was good reproducibility of this radiomic feature based on the blinded re-contouring, with little variation in the data between the two observers as shown in Fig. 4. The exception was two patient cases where the *wavelet_LHL_GLDZM_LILDE* feature showed some considerable differences, with higher values estimated from the contour generated by observer 2. The comparison of MTV for the contours of the different observers showed that the general contouring variability was low.

## 4. Discussion

In this analysis of 114 patients treated for oropharyngeal cancer we identified a radiomics risk signature based on the *wavelet_LHL_GLDZM_LILDE* image feature that was strongly associated with the risk of developing DM, specifically for patients with HPV p16-negative disease. As patients with HPV p16-negative disease are known to have a poor prognosis, further stratification of this group

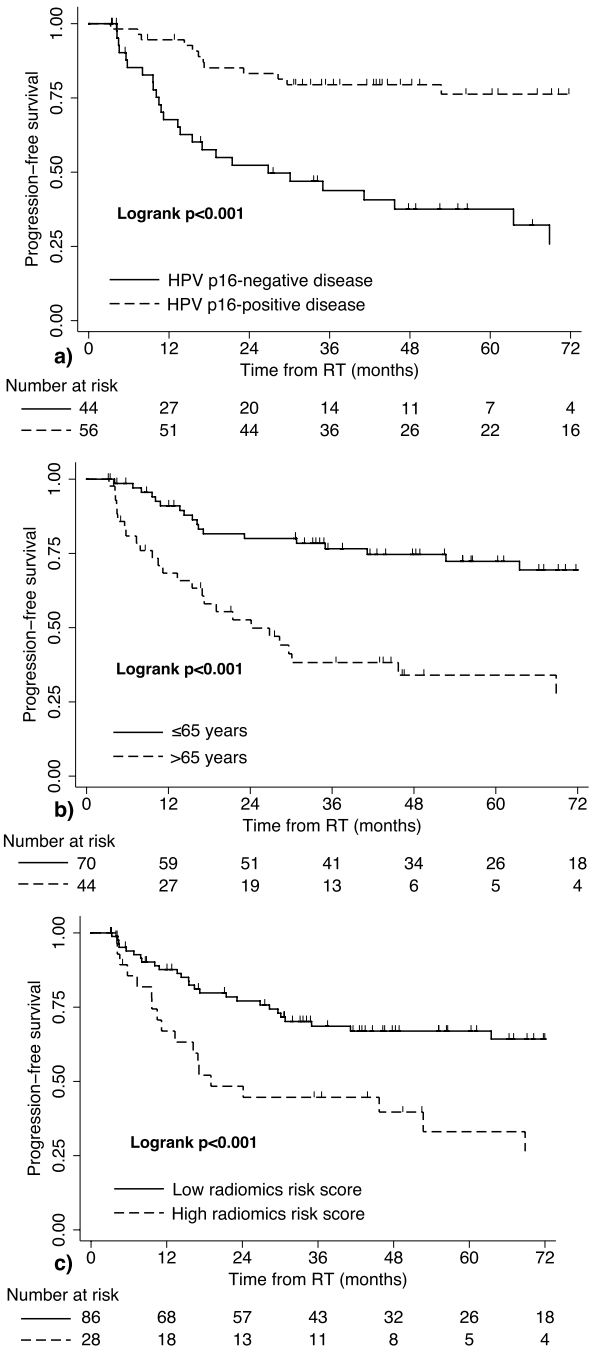


**Fig. 2.** Kaplan-Meier survival curves showing the association between progression-free survival and HPV p16 status (a), age (b) and radiomics risk score (c).

based on the risk of DM could provide an important avenue towards treatment adaptation with systemic options such as adjuvant immunotherapy for high-risk patients.

The radiomic image feature identified in this study was based on wavelet decomposition. In short, a wavelet transform decouples textural information in a manner akin to Fourier transforms, using low- and high-pass filtering. The nomenclature of e.g. "LHL" in a wavelet feature represents low-pass filtering in the x-direction, high-pass filtering in the y-direction and low-pass filtering in the z-direction. The *wavelet_LHL_GLDZM_LILDE* feature was generated based on the low-intensity large distance emphasis (LILDE) of the gray-level distance zone matrix (GLDZM), which describes the amount of homogeneous connected areas of low-intensity far from the edges of a volume [16]. This means that large connected areas of low values within the center of the tumor volume in the wavelet-transformed image would result in high values of the *wavelet_LHL_GLDZM_LILDE* feature. A potential correlate of a scenario with areas of low uptake towards the center could be hypoxia within a tumor volume, which has previously been shown to be associated with poor outcome [17]. It is important to note, however, that these characteristics of the identified radiomic feature refer to the wavelet-transformed image, and interpreting them in terms of the original PET image is not straightforward.

Identifying new biomarkers for patients with HPV p16-negative disease is especially important since much of the focus regarding treatment adaptation has been on treatment de-intensification for patients with HPV p16-positive disease, expected to have better treatment outcome. The need for novel treatment stratification options for patients with p16-negative disease is further exemplified in a recent study that found standard SUV metrics, specifically TLG, to be associated with disease-free survival only in patients with HPV-positive disease [12].

Previous studies have found radiomic features from PET and CT scans to be predictive of outcome for patients with OPC, with one study of 190 patients identifying shape, volume and textural features from the two modalities combined to be significant predictors of loco-regional progression in patients with HPV-associated OPC [18]. Another study of 174 patients with stage III-IV OPC found that MTV and tumor homogeneity were significantly associated with local failure, with features representing MTV, tumor solidity and kurtosis of the image intensity being associated with distant metastases, albeit borderline significant on independent validation [19]. However, that study did not have information about the HPV status of the patients' tumors. We did not find considerable improvement in predicting PFS when adding the radiomic feature to already established clinical predictors, and we also did not find any association with local failure based on our radiomics risk score stratification. The promising potential of the identified radiomics signature lies in the ability to stratify patients with HPV p16-negative disease into low- and high-risk of DM. This would nicely complement current clinical biomarkers for OPC as it would allow for further treatment individualization, for example by identifying patients most likely to benefit from novel systemic therapy strategies.

Limitations of our study include a relatively limited sample size of 114 patients from a single institution and the need for external validation to assess the generalizability to other patient cohorts. We used a random forest classification model to reduce the risk of potential overfitting, and also provided 5-fold cross-validated ROC AUCs with bootstrap bias-corrected confidence intervals to further mitigate this limitation. The z-score normalization and isotropic resampling of the PET data prior to analysis should also make the results less sensitive to variations in PET scanner and scanning protocol. The analysis based on a second observer redoing the semi-automatic tumor segmentations on the PET scans of a sub-group of 30 patients showed good reproducibility of the identified radiomic feature. We also did not perform HPV DNA testing since at our institution, p16 expression is routinely used as a surrogate for HPV status which is in line with most recent National Comprehensive Cancer Center guidelines, with HPV testing reserved for cases with equivocal or inconclusive findings.

In conclusion, we identified a radiomics risk signature strongly associated with the risk of distant metastases for patients with HPV p16-negative OPC. This could provide a promising avenue towards improved treatment stratification for these patients and the next important step would be to independently validate these results. This should ideally be done using a patient cohort from a different institution with varying treatment and diagnostic protocols, to ensure generalizability of the results.

## Conflicts of interest

None.

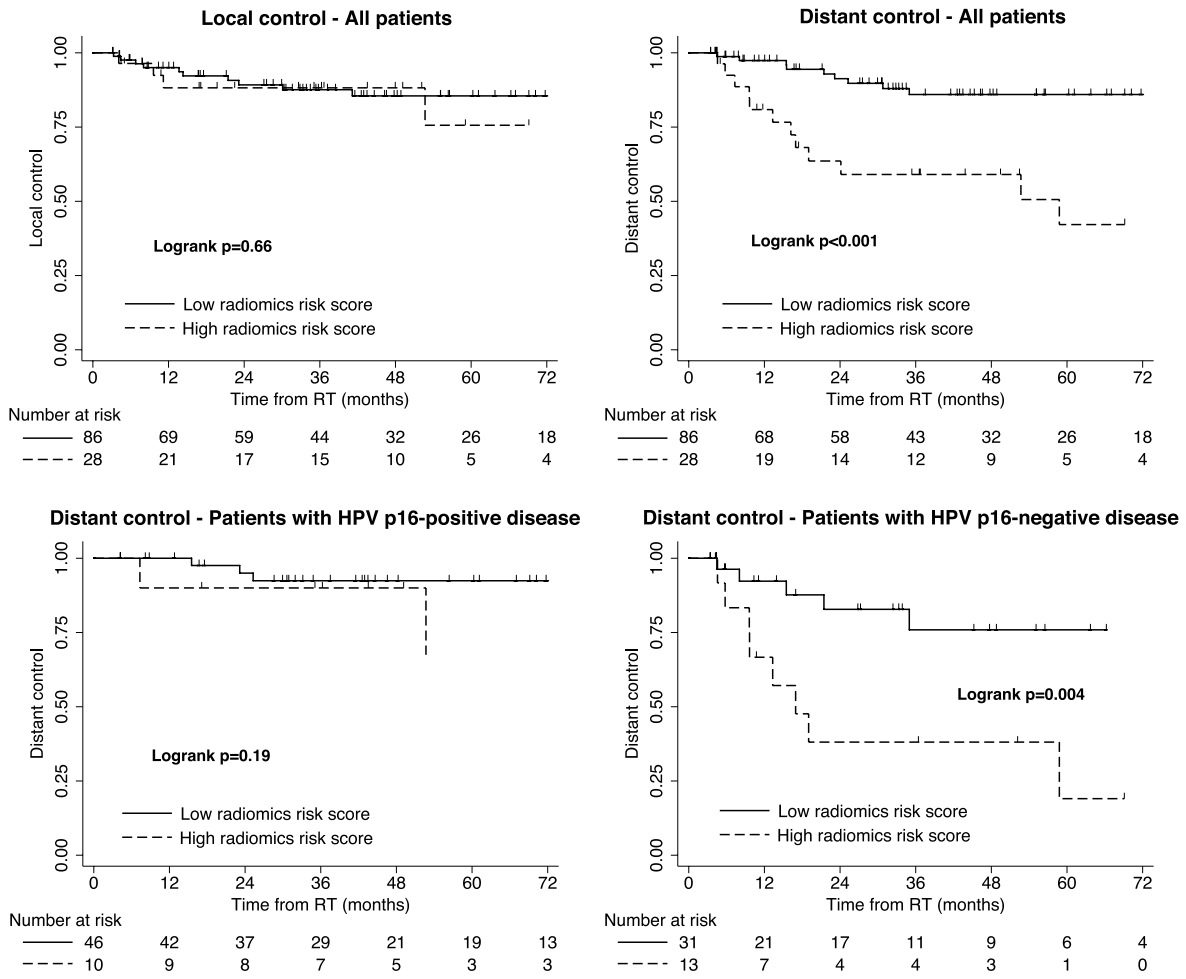


**Fig. 3.** Kaplan-Meier survival curves showing the difference between patients with low vs. high radiomics risk score for local control (a) and distant control (b). A sub-group analysis showing the comparison between low vs. high radiomics risk score for patients with HPV p16-positive disease (a) and those with HPV p16-negative disease (b).

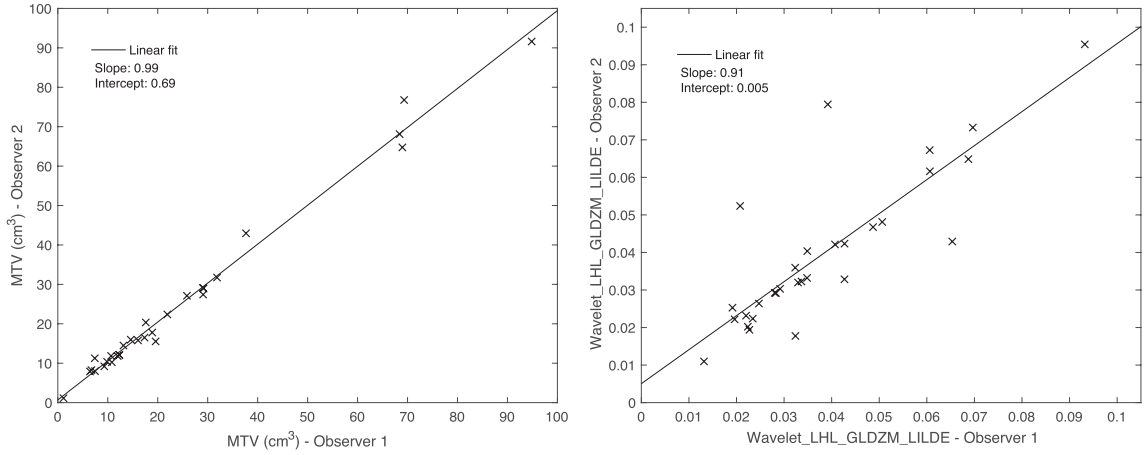


**Fig. 4.** The reproducibility of the tumor contours (metabolic tumor volume) and the wavelet_LHL_GLDZM_LILDE image feature is shown by comparing data from two different observers for a subset of 30 patients.

## Declaration of Competing Interest

The authors declare that they have no known competing financial interests or personal relationships that could have appeared to influence the work reported in this paper.

## Acknowledgements

An abstract based on preliminary results from this project was presented at ESTRO 2021.

## Appendix A. Supplementary data

Supplementary data to this article can be found online at https://doi.org/10.1016/j.phro.2022.02.005.

## References


[1] Fakhry C, Krapcho M, Eisele DW, D'Souza G. Head and neck squamous cell cancers in the United States are rare and the risk now is higher among white individuals compared with black individuals. Cancer 2018;124:2125–33.

[2] Gillison ML, Chaturvedi AK, Anderson WF, Fakhry C. Epidemiology of human papillomavirus-positive head and neck squamous cell carcinoma. J Clin Oncol 2015;33:3235–42.

[3] Ang KK, Harris J, Wheeler R, Weber R, Rosenthal DI, Nguyen-Tân PF, et al. Human papillomavirus and survival of patients with oropharyngeal cancer. N Engl J Med 2010;363:24–35.

[4] Ang KK, Zhang Q, Rosenthal DI, Nguyen-Tan PF, Sherman EJ, Weber RS, et al. Randomized phase III trial of concurrent accelerated radiation plus cisplatin with or without cetuximab for stage III to IV head and neck carcinoma: RTOG 0522. J Clin Oncol 2014;32:2940–50.

[5] Fakhry C, Zhang Q, Nguyen-Tân PF, Rosenthal DI, Weber RS, Lambert L, et al. Development and validation of nomograms predictive of overall and progression-free survival in patients with oropharyngeal cancer. J Clin Oncol 2017;35:4057–65.

[6] Denis F, Garaud P, Bardet E, Alfonsi M, Sire C, Germain T, et al. Final results of the 94–01 French Head and Neck Oncology and Radiotherapy Group randomized trial comparing radiotherapy alone with concomitant radiochemotherapy in advanced-stage oropharynx carcinoma. J Clin Oncol 2004;22:69–76.

[7] Nguyen-Tan PF, Zhang Q, Ang KK, Weber RS, Rosenthal DI, Soulieres D, et al. Randomized phase III trial to test accelerated versus standard fractionation in combination with concurrent cisplatin for head and neck carcinomas in the Radiation Therapy Oncology Group 0129 trial: long-term report of efficacy and toxicity. J Clin Oncol 2014;32:3858–67.

[8] Xiao C, Zhang Q, Nguyen-Tân PF, List M, Weber RS, Ang KK, et al. Quality of life and performance status from a substudy conducted within a prospective phase 3 randomized trial of concurrent standard radiation versus accelerated radiation plus cisplatin for locally advanced head and neck carcinoma: NRG oncology RTOG 0129. Int J Radiat Oncol Biol Phys 2017;97:667–77.

[9] Taghipour M, Sheikhbahaei S, Marashdeh W, Solnes L, Kiess A, Subramaniam RM. Use of 18F-fludeoxyglucose-positron emission tomography/computed tomography for patient management and outcome in oropharyngeal squamous cell carcinoma: a review. JAMA Otolaryngol Head Neck Surg 2016;142:79–85.

[10] Tsujikawa T, Narita N, Kanno M, Takabayashi T, Fujieda S, Okazawa H. Role of PET/MRI in oral cavity and oropharyngeal cancers based on the 8th edition of the AJCC cancer staging system: a pictorial essay. Ann Nucl Med 2018;32:239–49.

[11] Cheng N-M, Yao J, Cai J, Ye X, Zhao S, Zhao K, et al. Deep learning for fully automated prediction of overall survival in patients with oropharyngeal cancer using FDG-PET imaging. Clin Cancer Res 2021;27:3948–59.

[12] Gouw ZAR, La Fontaine MD, van Kranen S, van de Kamer JB, Vogel WV, van Werkhoven E, et al. The prognostic value of baseline 18F-FDG PET/CT in human papillomavirus-positive versus human papillomavirus-negative patients with oropharyngeal cancer. Clin Nucl Med 2019;44:e323–8.

[13] Mowery YM, Vergalasova I, Rushing CN, Choudhury KR, Niedzwiecki D, Wu Q, et al. Early (18)F-FDG-PET response during radiation therapy for HPV-related oropharyngeal cancer may predict disease recurrence. Int J Radiat Oncol Biol Phys 2020;108:969–76.

[14] Gillison ML, Trotti AM, Harris J, Eisbruch A, Harari PM, Adelstein DJ, et al. Radiotherapy plus cetuximab or cisplatin in human papillomavirus-positive oropharyngeal cancer (NRG Oncology RTOG 1016): a randomised, multicentre, non-inferiority trial. Lancet 2019;393:40–50.

[15] Mehanna H, Robinson M, Hartley A, Kong A, Foran B, Fulton-Lieuw T, et al. Radiotherapy plus cisplatin or cetuximab in low-risk human papillomavirus-positive oropharyngeal cancer (De-ESCALaTE HPV): an open-label randomised controlled phase 3 trial. Lancet 2019;393:51–60.

[16] Thibault G, Angulo J, Meyer F. Advanced statistical matrices for texture characterization: application to cell classification. IEEE Trans Biomed Eng 2014;61:630–7.

[17] Wegge M, Dok R, Nuyts S. Hypoxia and its influence on radiotherapy response of HPV-positive and HPV-negative head and neck cancer. Cancers (Basel) 2021;13.

[18] Haider SP, Sharaf K, Zeevi T, Baumeister P, Reichel C, Forghani R, et al. Prediction of post-radiotherapy locoregional progression in HPV-associated oropharyngeal squamous cell carcinoma using machine-learning analysis of baseline PET/CT radiomics. Transl Oncol 2021;14:100906.

[19] Folkert MR, Setton J, Apte AP, Grkovski M, Young RJ, Schöder H, et al. Predictive modeling of outcomes following definitive chemoradiotherapy for oropharyngeal cancer based on FDG-PET image characteristics. Phys Med Biol 2017;62:5327–43.